Colloid Polym Sci (2006) 284: 372–379
DOI 10.1007/s00396-005-1392-4

ORIGINAL CONTRIBUTION

Kiyoshi Shibata
Hiroshi Kimura
Akira Tsuchida
Tsuneo Okubo
Shohei Sato
Kohji Yoshinaga

Electro-optic effects of colloidal crystals of polymer-modified silica spheres immobilized with gelator

Received: 25 March 2005
Accepted: 28 July 2005
Published online: 23 September 2005
© Springer-Verlag 2005

K. Shibata · H. Kimura · A. Tsuchida (✉)
Department of Applied Chemistry,
Faculty of Engineering,
Gifu University, 1-1 Yanagido,
Gifu 501-1193, Japan
E-mail: tsuchida@apchem.gifu-u.ac.jp
Tel.: +81-058-2932624
Fax: +81-058-2301893

T. Okubo
Institute for Colloidal Organization,
3-1-112 Hatoyama, Uji Kyoto
611-0012, Japan

T. Okubo
Cooperative Research Center,
Yamagata University,
4-3-16 Jonan, Yonezawa
Yamagata 992-8510, Japan

S. Sato · K. Yoshinaga
Department of Applied Chemistry,
Faculty of Engineering,
Kyushu Institute of Technology,
1-1 Sensui, Tobata
Kitakyusyu 804-8550, Japan

Abstract Electro-optic responses of colloidal crystals consist of poly(maleic anhydride-*co*-styrene)-modified silica spheres (P(MA-ST)/SiO_2) in acetonitrile and the crystals immobilized with a gelator, *N*-benzyloxycarbonyl-*L*-isoleucilaminooctadecane (Z-L-Ile-C-18), are studied by reflected-light intensity measurements and time-resolved reflection spectroscopy. Application of an alternating electric field deforms P(MA-ST)/SiO_2 crystal lattices reversibly. The response waveforms from the crystals are dependent on the frequency and strength of the applied electric field; similar dependencies have been qualitatively observed for the colloidal crystals consisting of polystyrene or silica spheres in aqueous media in our previous studies. Both gelated and ungelated P(MA-ST)/SiO_2 crystals change the reflection intensity, however, the amplitude is larger for the latter. The small response for the gelated P(MA-ST)/SiO_2 crystals is attributed to the higher elastic modulus (G). The G value of the gelated P(MA-ST)/SiO_2 crystals in acetonitrile is estimated from the change in the inter-sphere distance to be 8.0 Pa, which is about 2.3 and 2.4 times larger than that for ungelated P(MA-ST)/SiO_2 crystals in acetonitrile and colloidal silica crystals in aqueous media, respectively.

Keywords Colloidal crystal · Electro-optic effect · Immobilization · Gelator · Bragg reflection · Reflection spectra

Introduction

When a suspension of monodispersed colloidal spheres is deionized exhaustively in polar solvents such as water, a crystal-like structure is formed [1–5]. This colloidal crystal is formed by the extended electrical double layers around the spheres and by the Brownian motion of the spheres. Many researchers have studied the physical properties of colloidal crystals in aqueous and organic solvents [1–15]. The thickness of the electrical double layers is approximated with the Debye-screening length, D_l, given by

$$D_l = \left(\frac{4\pi e^2 n}{\varepsilon k_B T}\right)^{\frac{-1}{2}} \tag{1}$$

where ε is the electronic charge, ε the dielectric constant of solvent, k_B the Boltzmann constant, T the absolute temperature, and n the concentration of free-state cations and anions in suspension, given by $n = n_c + n_s +$

n_o, where n_c is the concentration (number of ions per cubic centimeter) of diffusible counterions, n_s is the concentration of foreign salt, and n_o is the concentration of both H^+ and OH^- from the dissociation of water. In order to estimate n_c, the fraction of free-state counterions (β) must be known. Note that the maximum value of D_l observed hitherto was ca 1 μm in water. The similar value of D_l, i.e., 1.2 μm, is also estimated from Eq. 1 by taking $n_o = 2\times10^{-7}$ (mol/dm^3) $\times N_A \times10^{-3}$ (cm^{-3}), where N_A is Avogadro's number. It should be mentioned here that β values are very small for typical colloidal particles, and the n values calculated using the stoichiometric charge number (Z) on a colloidal surface (instead of βZ) is always overestimated. In comparison with water, organic solvents have smaller n and ε values. In the previous report, the critical concentration of melting (ϕ_c, in volume fraction) for the colloidal crystal was around 0.0002 in pure water and increased sharply as the fraction of organic solvents increase [16]. The change in ϕ_c is explained well with the change in ϵ of solvent mixtures. Recently, colloidal crystallization at comparatively lower volume fraction ($\phi \leq 0.02$) in organic solvents has been succeeded for silica sphere and polymer-modified silica spheres [16, 17]. In the latter case, the organic solvents must be polar and good solvents for the grafted polymer on the sphere surface. The crystals thus formed are stable and are found to have face-centered cubic (fcc) and body-centered cubic (bcc) structures in crystal lattice, similar to the colloidal crystals in water.

The elastic modulus of typical colloidal crystals in the polar solvents is very small (10^{-2}–10^3 Pa) when compared with that of metals (10^{11}–10^{12} Pa), and the colloidal crystals are easily melted by external forces such as electric field and gravity etc [4]. Therefore, the incorporation of the colloidal crystal structure into a polymer matrix is an important technique for the application of new functional materials, and immobilization of colloidal crystals by gelation especially attracts a lot of attention. Thus far, gelation by photopolymerization has been generally used, e.g., Asher et al. [18, 19] succeeded to form cross-linked hydrogel network by acrylamide monomer with a cross-linker bisacrylamide and a photoinitiator. In recent years, the low molecular-weight gelators have been extensively invented and many thermal reversible gels, i.e. physical gels, have been formed [20]. In the present article, by the addition of this type of gelator, the 'gelated crystals' immobilizing the colloidal crystals are obtained, and their electro-optic properties are studied.

When colloidal crystals are formed in a polar solvent, the lattice spacing changes sensitively by the application of an external electrical field, due to the repulsive and long-range inter-sphere force between the constituent colloidal particles [10, 21–31]. When an electric field is applied to a colloidal suspension, the negatively charged colloidal particles, in most cases, are attracted to the anode electrode and the inter-sphere lattice spacing becomes short at this side. On the other hand, the particles are repelled from the cathode electrode, and then the inter-sphere distance becomes long at the cathode. Because the lattice spacing in the colloidal crystal matches with the wavelength range of visible light, the deformation of the crystal lattices in the electric field can be observed from the change in the peak wavelength of the Bragg reflection [30, 32–34]. It is possible to modulate incident light intensity by the application of an electric field to the colloidal crystals. These phenomena are called electro-optic effects [35, 36] in the broad sense of the term and the authors have studied the properties in detail. Significant modulation effects are observed in the phase difference, waveform transformation and harmonic generation, for example [37–39]. The colloidal crystals also show the electric potential storage ability as an electric energy capacitor [40].

Though the efficient electro-optic effects, which require the large deformation of the crystals, may contradict the immobilization of the crystals, the gelation of colloidal crystals is an attractive technique from the viewpoint of material science. The electro-optic effects of the colloidal crystals of poly(maleic anhydride-*co*-styrene)-modified silica spheres (P(MA-ST)/SiO_2) gelated by *N*-benzyloxycarbonyl-*L*-isoleucilaminooctadecane (Z-L-Ile-C-18) in acetonitrile are studied in this paper.

Experimental

Materials

The composite particles of P(MA-ST)/SiO_2 were synthesized according to the method previously reported [17]. A suspension of ethanolic monodisperse colloidal silica (6 ml, Catalyst and Chemicals), containing 15 wt% SiO_2 spheres of 135 ± 4 nm diameter, was added to trimethoxysilyl-terminated poly(MA-ST)s (1.5 g, P(MA-ST)-Si(OMe)$_3$) in tetrahydrofuran (5 mL, Wako), and then 1,2-dimethoxyethane (50 mL, Wako) was added to the mixture. The suspension was stirred at 90°C and 45 mL of 1,2-dimethoxyethane was removed by azeotropic distillation. Then, 10 mL of tetrahydrofuran was added and the mixture was refluxed overnight at 70°C. Centrifugal separation from the suspension in acetone was carried out eight times to remove unreacted polymer silane, and drying under reduced pressure gave the composite P(MA-ST)/SiO_2 particles. Using thermogravimetric analysis (TGA-50, Shimadzu), the amount of the attached polymer was determined to be 57 mg/g-SiO_2. As the number-average molecular weight (M_n) of the attached polymer is 7,100, the square root of mean-square end-to-end distance $< R^2 >^{1/2}$ was calculated to be 2.3 nm, assuming the freely rotating chain molecular model.

The gelator Z-L-Ile-C-18 was synthesized as follows. *N*-Benzyloxycarbonyl-*L*-isoleucine (0.50 g, Z-L-Ile, Aldrich) was dissolved in distillated ethyl acetate (5 mL, Wako). *N*, *N′*-Dicyclohexylcarbodiimide (0.43 g, DCC, Wako) was added to the mixture, and stirred for 30 min at 0°C. Then, stearylamine (0.51 g, Wako) was added to the mixture, and stirred for 1 h at 0°C. The mixture was further stirred for 12, 10 and 3 h at 35, 45 and 60°C, respectively. The insoluble residual DCC-urea was removed from the mixture by heating filtration. The filtrate was cooled, and formed a gel. The gel was filtered with suction, and the residual gel was dissolved in overheating distillated ethyl acetate. The solution was cooled and the gel formed was dried under a reduced pressure, giving the gelator Z-L-Ile-C-18. Figure 1 shows the structural formulae of the polymer-modified sphere and the gelator used in this study.

Monodispersed colloidal silica spheres (CS91, Catalyst and Chemical Ind. Co.) in an aqueous suspension are comparable in their size (110 nm in diameter) to that of P(MA-ST)/SiO_2 (135 nm). The sphere sample was treated with a mixed bed of anion- and cation-exchange resins (AG501-X8(D), Bio-Rad Lab.) for more than 10 years in order to delete ionic impurities as completely as possible.

Sample preparation

Table 1 shows the constitution of the three samples measured in this study. To obtain the ‘ungelated’ colloidal crystals, i.e. the crystals without gelator in acetonitrile (Code#2 in Table 1), first the dispersion of composite particles of P(MA-ST)/SiO_2 in acetonitrile and subsequently centrifugal separation were carried out. Next the particles were dispersed in acetonitrile again under sonication. The ‘gelated’ colloidal crystals were obtained by the addition of the gelator Z-L-Ile-C-18 (0.4 wt%) into the ‘ungelated’ colloidal crystals. The gelator was dissolved at 60°C, and the subsequent cooling to the room temperature gave the gelated colloidal crystals (#1). These crystals showed bright iridescent colors by irradiation of white light.

For the purpose of comparison with the colloidal crystals of P(MA-ST)/SiO_2 spheres, those of CS91 spheres in water were prepared (#3). The nearest-neighbor inter-sphere distance of the silica colloidal crystals was adjusted to be almost equal to those of P(MA-ST)/SiO_2 colloidal crystals. The inter-sphere distance of colloidal crystals can be calculated using Eqs. 2 and 3 [42, 43].

$$l_0 = 0.904\, d_0\, \phi^{-1/3} \tag{2}$$

$$l_{obs} = 0.6124\, \lambda_p\, n_r^{-1} \tag{3}$$

where l_0 is the distance calculated from the sphere diameter (d_0) and the volume fraction (ϕ), l_{obs} is the distance determined from the Bragg peak wavelength (λ_p) and the refractive index of the suspension (n_r). The values of n_r are approximated to those of acetonitrile (1.344) and water (1.333) in this work. In the case of P(MA-ST)/SiO_2 crystals of $\phi = 0.130$, the Bragg peak appeared at $\lambda_p = 550$ nm. The values of l_0 and l_{obs} are calculated to be 241 and 251 nm, respectively. The difference between l_0 and l_{obs} is considered to be caused by the avoidence of the exclusion volume effect of the grafted polymer chains around the core of P(MA-ST)/SiO_2 particles. The d_0 value must include the polymer chain length, i.e. the thickness of the polymer layer. If we add 4.6 (=2.3×2) nm polymer layers at the maximum to the d_0 of P(MA-ST)/SiO_2 particles, the l_0 is calculated to be 249 nm, and both l_0 and l_{obs} agreed within experimental error. The thickness of the electrical double layers D_{obs} (= (l_{obs}–d_0)/2) is calculated to be about 56 nm, whereas the thickness of the polymer layers is 2.3 nm. Evidently, the colloidal crystals of P(MA-ST)/SiO_2 spheres are formed by the electrical repulsion between the extended electrical double layers around the spheres.

The concentration of reference aqueous suspension of CS91 spheres was determined from λ_p of the P(MA-ST)/SiO_2 suspension assuming $l_0 = l_{obs}$ in this work. The ion-exchange resins were removed from the suspension when the sample was poured into observation cell. Water used in these experiments was the purest one obtained from Milli-Q water system (Milli-RO Plus and Milli-Q Plus. Millipore Ltd).

Electro-optic measurements

Inside two parallel walls of the observation optical cell (inner size: 2 or 5 mm (optical path

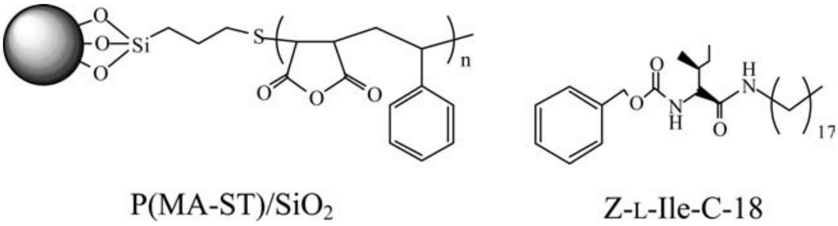

Fig. 1 Structures of poly(maleic anhydride-*co*-styrene)/SiO_2 (P(MA-ST)/SiO_2) and the gelator (Z-L-Ile-C-18)

Table 1 Constitution of the samples

Code	Particles	d_0 (nm)	ϕ	Solvent	Gelator
# 1	P(MA-ST)/SiO_2	135	0.130	Acetonitrile	[Z-L-Ile-C-18]
# 2	P(MA-ST)/SiO_2	135	0.133	Acetonitrile	–
# 3	CS91	110	0.061	Water	–

length)×10 mm×48 mm) were coated with transparent electrical conducting NESA membrane ($<10\ \Omega\ cm^{-1}$). An oscillator (FG110, Yokogawa, or WF1941, NF) was used to apply a sinusoidal electric field to the transparent electrodes. Figure 2 shows the schematic representation of the instruments. A light beam from a halogen light source (PHL-50, Sigma Koki) was introduced into a Y-type optical fiber and was focused on the inside cell wall (<1.5 mm diameter). The incident light beam was parallel to the electric field in the cell. Intensity change of the reflected light was detected by a photomultiplier (R649, Hamamatsu Photonics, Hamamatsu) and then recorded on a digital oscilloscope (HP54810A, Hewlett Packard, CO, USA) for the intensity measurements. Time-resolved reflection spectra were taken on a photonic multichannel analyzer (PMA-50, Hamamatsu Photonics). All the measurements were made in an air-conditioned room at 25 ± 1°C.

Results and discussion

Reflection intensity measurements

Figure 3 shows typical examples of the waveforms of reflected light intensity when a sinusoidal electric field was applied to the crystals. Curves (a–d) are the reflection signals from gelated crystals (#1 in Table 1) in 2 mm cell, in 5 mm cell, ungelated crystals (#2) in 2 mm cell and in 5 mm cell, respectively. The bottom curve (e) shows a waveform of the applied electric field. The ordinate of curve (d) is reduced to 1/3 due to the larger amplitude. Clearly, the reflection intensities from the crystals were modulated substantially and periodically. Though these results are similar to those for the colloidal crystals in water [30, 32–34], amplitude and shape of the waveforms are different. The reflection amplitude from the gelated crystals was smaller than that from ungelated crystals; the amplitudes of curves (c) and (d) were three and seven times larger than those of (a) and (b), respectively. The waveform of the ungelated crystals showed two peaks within a period of one sinusoidal cycle. This is attributed to the higher-order harmonics generation caused by the nonlinear and viscoelastic electro-optic response of the crystal lattices [38]. The harmonics generation has often been observed also for the aqueous suspension systems [30, 31, 33]. On the other hand, the gelated crystals showed practically no harmonic generation in these experimental conditions. This is probably due to the restricted lattice deformation by the immobilization of the crystals. In Fig. 3, a long optical path length gave large reflection amplitude for both gelated and ungelated samples. This result implies the existence of a significant wall effect; i.e., the movement of spheres in the crystal cages is restricted in the region close to the cell wall [33]. The reflection waveforms in Fig. 3 clearly show also the existence of phase delay when they are compared with the applied signal, which supports the viscoelastic nature of the colloidal crystals. The values of phase delay changed by the gelation and the optical path length owing to the different resonance modes of the crystal lattices.

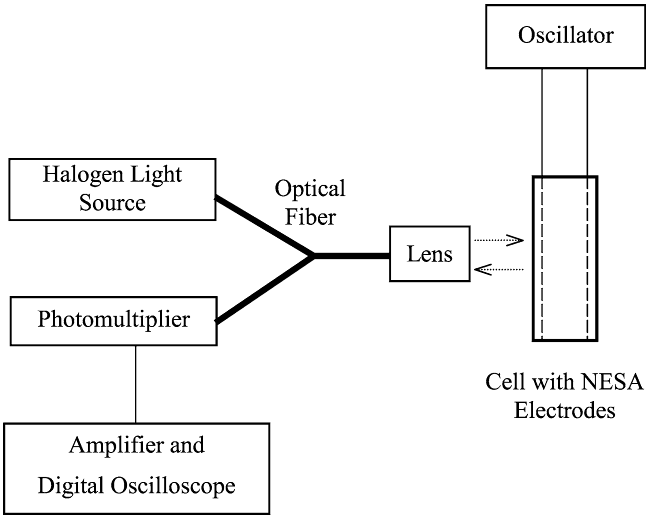

Fig. 2 Schematic representation of the apparatus for electro-optic measurements of colloidal crystals

The response waveforms were strongly dependent on the frequencies and voltages of the applied sinusoidal wave. Amplitude (A) and phase difference (φ) for the reflection waves were determined from the intensity difference between the maximum and minimum intensities and the time difference between two positive peaks of applied and response waveforms, respectively [38]. As shown in Fig. 3 no appreciable harmonic component appeared for the gelated crystals.

Figures 4a and b show the frequency (f) dependencies of A and φ values of the reflected responses, respectively, at the constant electric field of 2 V cm^{-1}.

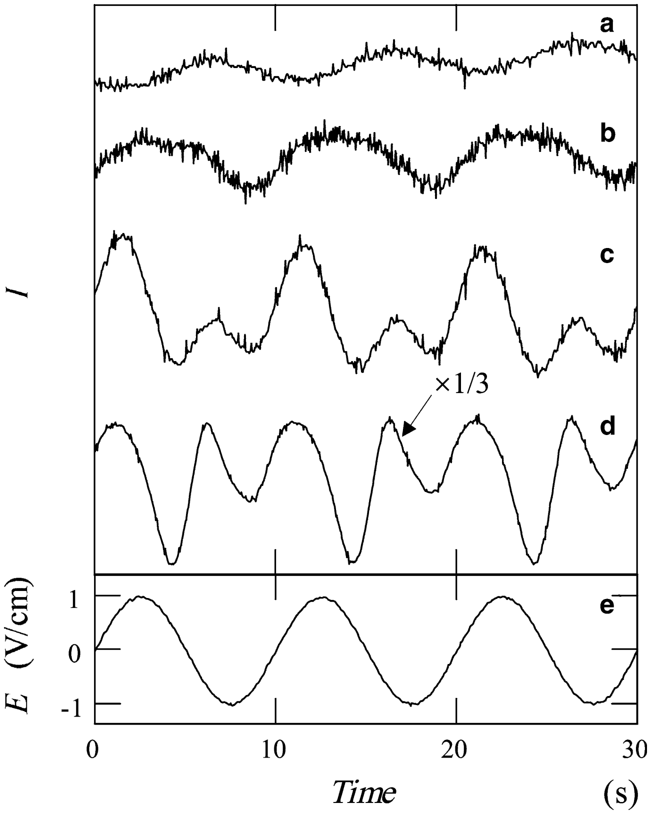

Fig. 3 Waveforms of reflected light intensity (a–d) and applied sinusoidal electric field (e) for the colloidal crystals of P(MA-ST)/SiO_2 with gelator (#1 in Table 1) in 2 mm cell (a) and 5 mm cell (b), P(MA-ST)/SiO_2 without gelator (#2) in 2 mm cell (c) and 5 mm cell (d), at 25°C, f = 0.1 Hz, E = 2 V/cm^{-1}

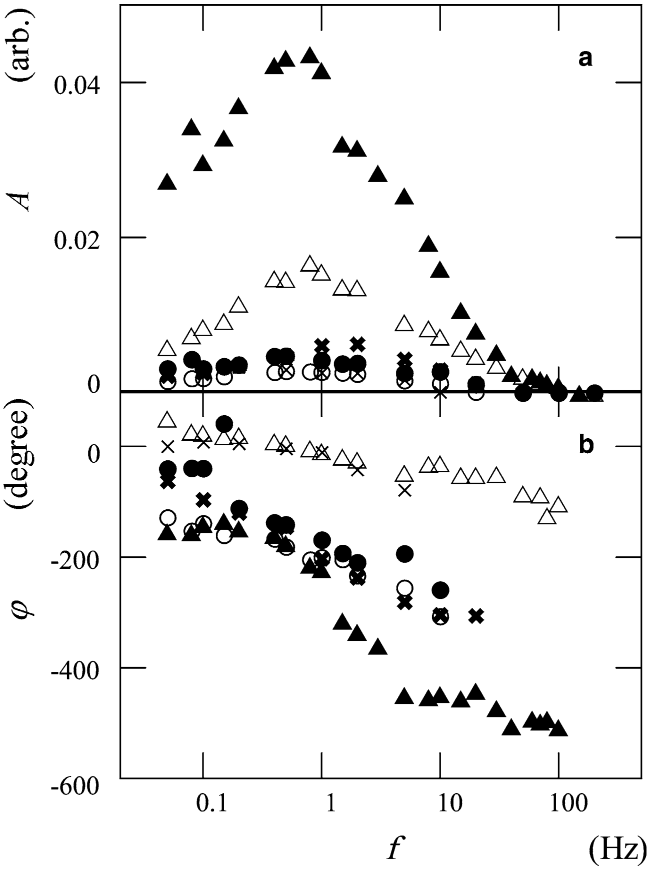

Fig. 4 Amplitudes (a) and phase differences (b) in the reflection signals for colloidal crystals when a sinusoidal electric field is applied at 25°C, E = 2 V/cm. P(MA-ST)/SiO_2 with gelator in 2 mm cell (*open circle*) and 5 mm cell (*filled circle*), P(MA-ST)/SiO_2 without gelator in 2 mm cell (*open triangle*) and 5 mm cell (*filled triangle*), CS91 (#3 in Table 1) in 2 mm cell (×) and 5 mm cell (**×**)

The values of A for the ungelated crystals were larger than those for the gelated crystals throughout all the frequency range, and the response was obtained up to 100 Hz. The 5 mm cell gave the larger A values than those for 2 mm cell. These results are reasonable, because the spheres in gelated crystals are difficult to move. It is interesting that P(MA-ST)/SiO_2 spheres gave the largest A values at around f = 0.8 Hz, regardless of the presence of gelator and the thickness of the cells. Stoimenova et al. [43] pointed out the existence of resonance frequencies for colloidal crystals in aqueous media; in their cases the resonance frequencies increase according to the increase in sphere concentration. However in Fig. 4, the maximum A values were the same irrespective of the system. Therefore in the present case, the decrease in A at the low frequency range ($<$0.8 Hz) must be caused by the partial melting of the colloidal crystals due to the pseudo-steady state application of the low frequency electric field [40]. On the other hand, the decrease of A at the high frequency range ($>$0.8 Hz) will be caused by the slow response of the crystals in comparison with the change of applied electric field [32]. The A values for the reference CS91 colloidal crystals in water (#3) are also shown in Fig. 4a, and they are similar order to those for the gelated crystals. On the other hand, A values for the ungelated crystals are larger than those for CS91 and gelated crystals. These results show the higher elastic modulus for the gelated crystals than that for the ungelated crystals. As for the phase differences (φ), the value was decreased substantially when f increased for all the systems. These results are consistent with the previous reports [31–33, 37].

Figures 5a and b show the electric field (E) dependencies of A and φ values, respectively. The value of A increased linearly when E increased, irrespective of the thickness of cells and the kinds of spheres. The higher E value is considered to cause a larger deformation of the crystals. These results are the same as our previous reports on silica crystals [33, 37]. It is highly plausible that the viscoelastic nature of the colloidal crystals causes the phase delay.

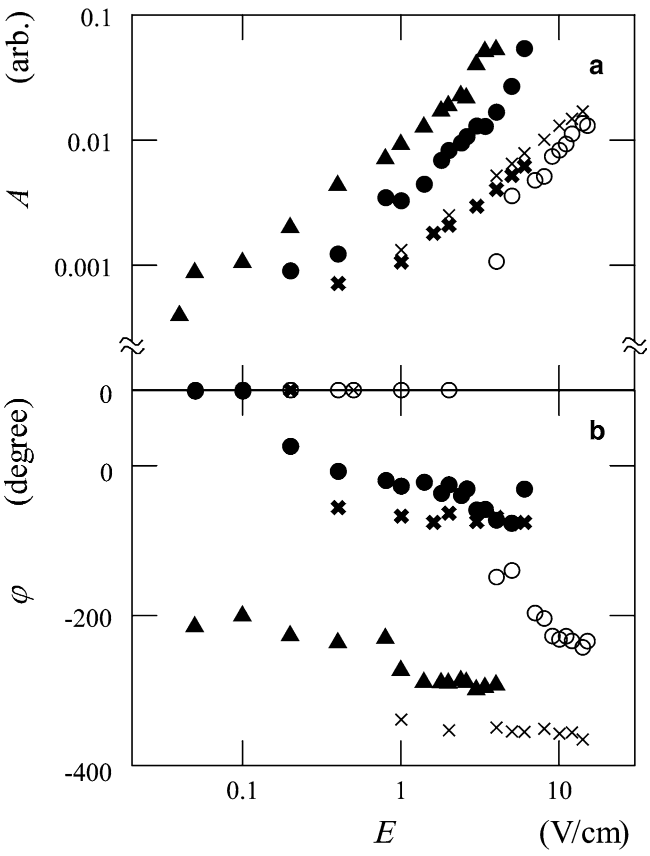

Fig. 5 Amplitudes (**a**) and phase differences (**b**) in the reflection signals for colloidal crystals when a sinusoidal electric field is applied at 25°C, $f = 0.05$ Hz. P(MA-ST)/SiO_2 with gelator in 2 mm cell (*open circle*) and 5 mm cell (*filled circle*), P(MA-ST)/SiO_2 without gelator in 5 mm cell (*filled triangle*), CS91 in 2 mm cell (×) and 5 mm cell (**×**)

Time-resolved reflection spectroscopy

When an electric field is applied to the colloidal crystals of P(MA-ST)/SiO_2 spheres in acetonitrile, the electro-optic effects are caused by the movement of the spheres (i.e. deformation of the crystal lattices), as well as reference CS91 colloidal crystals in water. It is possible to estimate the inter-sphere distance of the crystals directly from the Bragg peak wavelength of the reflection spectra. Figure 6 shows the time-resolved reflection spectra for the crystals of P(MA-ST)/SiO_2 spheres. Figure 6 indicates the Bragg peaks in their largest shift because the change in the Bragg peak was dependent on the applied frequency. Figures 6a and c show the spectra for the gelated crystals (#1), and Figs. 6b and d show those for the ungelated crystals (#2). The heavy curves indicate the spectrum obtained in the absence of electric field, and the maximum intensities of them were larger for the ungelated crystals. This is because the nearest inter-sphere distance for the ungelated crystals is approximately constant, whereas that for the gelated crystals get out of order owing to the shrinkage accompanied with the gelation reaction. In Fig. 6, reflection spectra 1–5 are recorded within one cycle of applied sinusoidal wave. The peak was blue (1–3) and red (3–5) shifted according to positive and negative potentials of the electrode, respectively. These results are the same as these for the CS91 colloidal crystals in water. Because the surface of polymer-modified spheres is negatively charged as well as CS91 spheres, the inter-sphere distance at positive electrode becomes short and long by the application of positive and negative electric field, respectively. The large peak shift was observed for the ungelated crystals and in the 5 mm cell, whose results were consistent with those of reflection intensity measurements as described before.

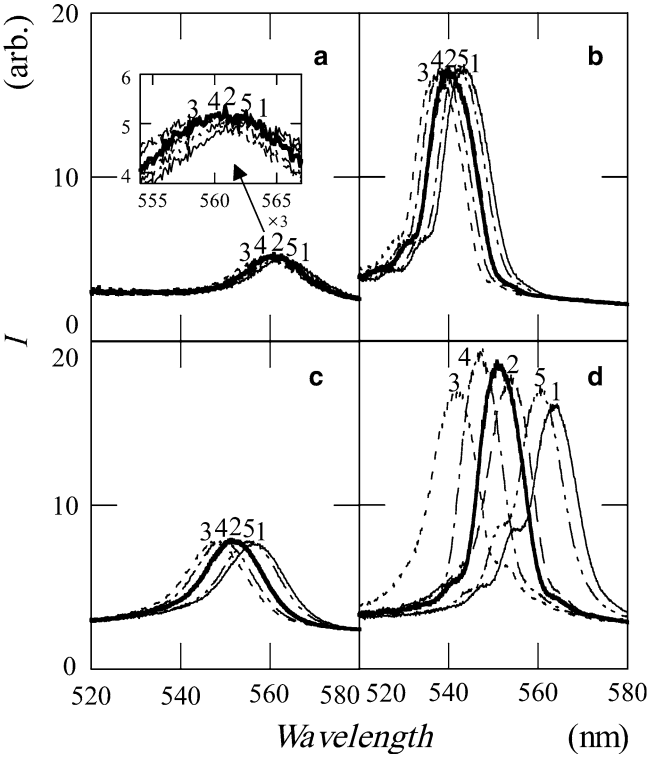

Fig. 6 Time-resolved reflection spectra for P(MA-ST)/SiO_2 with gelator in 2 mm cell (a), without gelator in 2 mm cell (b), with gelator in 5 mm cell (c) and without gelator in 5 mm cell (d) when a sinusoidal electric field is applied at 25°C. 1:$/T = 0$, 2:0.24, 3:0.52, 4:0.68, 5:0.88. $E = 2$ V/cm, $f = 1$ Hz (**a**), 0.5 Hz (**b**), 0.05 Hz (**c**), 0.2 Hz (**d**). Bold curves $E = 0$ V cm^{-1}

Inter-sphere distances divided by those in the absence of electric field (l_{obs}/l) are calculated using Eq. 3 and plotted against time in Fig. 7. The abscissa, t/T, is the time t divided by T, the period for one cycle of the applied sinusoidal wave. Clearly, l_{obs}/l changed periodically by the application of sinusoidal wave to the crystals. The ranges of l_{obs}/l variation ($\Delta l_{obs}/l$) were

0.007, 0.012, 0.017 and 0.039 for the gelated crystals in 2 mm cell, ungelated crystals in 2-mm cell, gelated crystals in 5 mm cell and ungelated crystals in 5 mm cell, respectively.

Figure 8 shows the frequency (*f*) dependencies of $\Delta l_{obs}/l$. The $\Delta l_{obs}/l$ values measured in 2 mm cell were smaller than those in 5 mm cell. The maximum $\Delta l_{obs}/l$ values in 2-mm cell appeared at almost the same frequency as ca. 1 Hz. On the other hand, those in 5 mm cell varied, i.e., < 0.05 Hz for the gelated crystals, ca. 0.1 Hz for the ungelated crystals and ca. 2 Hz for the reference CS91 crystals in water. The reference CS91 crystals gave maximum response at ca. 1–2 Hz for the reflection intensity measurements in 5-mm cell as shown in Fig. 4. This frequency range corresponded well to that measured by time-resolved reflection spectra, as shown in Fig. 8. However, the crystals of polymer-modified particles gave different frequencies for the maximum response according to the measurement methods as shown in Figs. 4 and 8. This discrepancy is attributed to the nonlinearity between $\Delta l_{obs}/l$ and the reflection intensity, probably caused by large strain of P(MA-ST)/SiO_2 crystals lattices and partial melting of the crystals by the application of large external electric field. The order of largest $\Delta l_{obs}/l$ values was #1 $<$#2 ~#3 for three systems in Table 1. The change of inter-sphere distance for the gelated crystals was small and ca. 1/3 times than that for the ungelated crystals.

As mentioned earlier, the optical response for the gelated crystals is smaller than that for the ungelated crystals. The optical response of crystals is dependent on the sphere mobility in an electric field, i.e. hardness of colloidal crystals (elastic modulus of the crystals). It is possible to estimate the elastic modulus (*G*) of the gelated crystals by the comparison of $\Delta l_{obs}/l$ under the same electric field. In this work, however, the melting of colloidal crystals of the P(MA-ST)/SiO_2 spheres is observed at low frequency range of the applied electric field. Therefore the comparison of $\Delta l_{obs}/l$ was made at the largest values. In our previous reports, the *G* value of the colloidal crystals of CS91 spheres (ϕ = 0.129) was determined to be 7.0 Pa from the slope in the stress-strain curve [44]. In the present study, the *G* value of CS91 crystals (ϕ = 0.061) is estimated to be ca. 3.3 Pa, because the value of *G* is proportional to the number of spheres in a unit volume of suspension (*N*) [5]. All the systems in this study give to similar in *N* values. Consequently, *G* values of the gelated and ungelated P(MA-

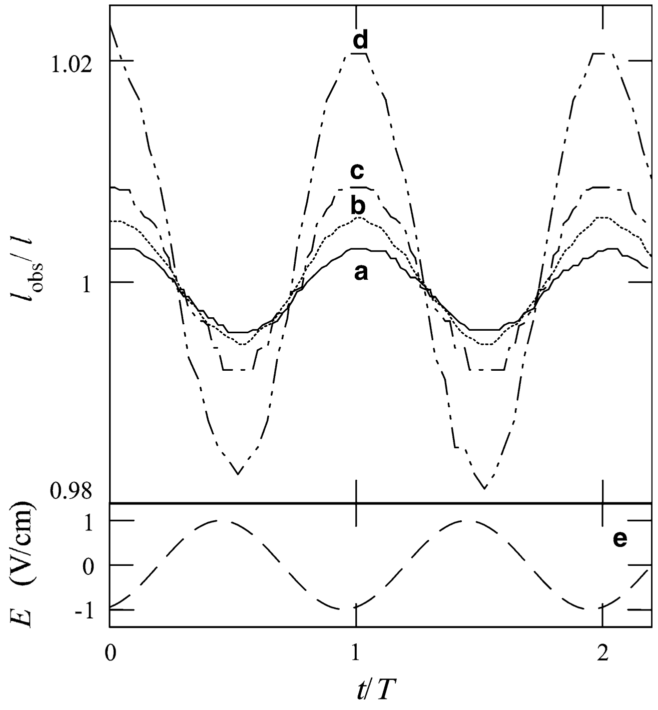

Fig. 7 Inter-sphere distance divided by that in the absence of electric field (l_{obs}/l) for the colloidal crystals of P(MA-ST)/SiO_2 with gelator in 2 mm cell (a, *f* = 1 Hz), without gelator in 2 mm cell (b, 0.5 Hz), with gelator in 5 mm cell (c, 0.05 Hz) and without gelator in 5 mm cell (d, 0.2 Hz) when a sinusoidal electric field (e) is applied at 25°C, E = 2 V/cm

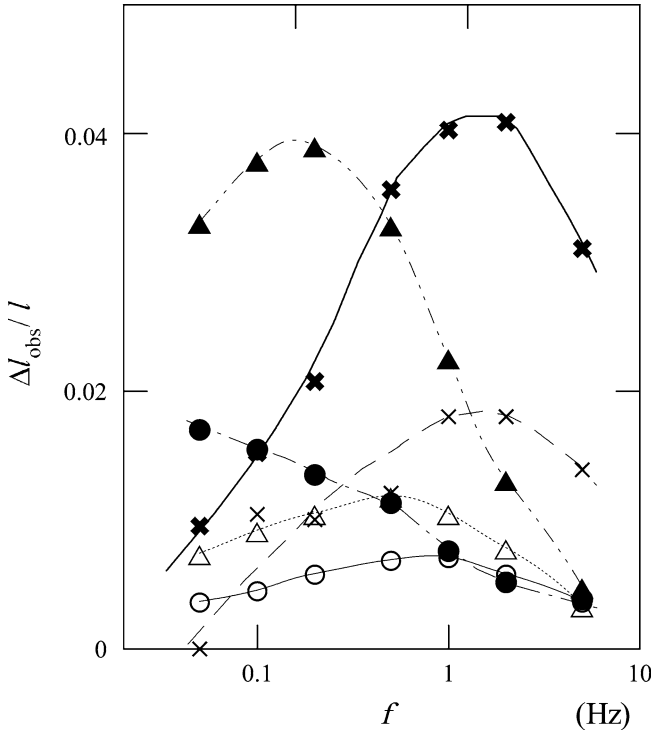

Fig. 8 Change in the inter-sphere distance divided by that in the absence of electric field ($\Delta l_{obs}/l$) for colloidal crystals when a sinusoidal electric field is applied at 25°C, E = 2 V cm^{-1}. P(MA-ST)/SiO_2 with gelator in 2 mm cell (*open circle*) and 5 mm cell (*filled circle*), P(MA-ST)/SiO_2 without gelator in 2 mm cell (*open triangle*) and 5 mm cell (*filled triangle*), CS91 in 2 mm cell (×) and 5 mm cell (**×**)

ST)/SiO$_2$ crystals in this study are estimated to be 8.0 and 3.5 Pa, respectively, from their $\Delta l_{obs}/l$ values. The G values were in the order #3 ~#2 < #1.

Conclusion

Electro-optic responses of gel-immobilized colloidal crystals of P(MA-ST)/SiO$_2$ spheres were observed in acetonitrile. The optical responses of the colloidal crystals of polymer-modified P(MA-ST)/SiO$_2$ spheres without gelator were dependent on f and E of the applied electric field qualitatively in the same manner as those of silica colloidal crystals in water. On the other hand the immobilization of the crystals by gelation attenuated the electro-optic responses. The G value of the gelated crystals was estimated to be 8.0 Pa, which is 2.3 and 2.4 times larger than those for ungelated and silica crystals, respectively.

Acknowledgements Drs. M. Komatsu and Dr. M. Hirai of Catalyst & Chemical Ind. Co. (Tokyo) are thanked deeply for their providing the sample of the colloidal silica spheres. This research was partially supported by the Ministry of Education, Science, Sports and Culture, Grant-in-Aid for Scientific Research (B), 60183076, 2004.

References

1. Vanderhoff W, van de Hul W, Tausk RJM, Overbeek JThG (1970) In: Goldfinger G (ed) Clean surfaces: Their prepararion and characterization for interfacial studies. Dekker, New York
2. Pieranski P (1983) Contemp Phys 24:25
3. Ottewill RH (1985) Ber Bunsen Phys Chem 89:281
4. Okubo T (1988) Accounts Chem Res 21:281
5. Okubo T (1993) Prog Polym Sci 18:481
6. Hiltner PA, Papir YS, Krieger IM (1971) J Phys Chem 75:1881
7. Kose A, Ozaki M, Takano K, Kobayashi Y, Hachisu S (1973) J Colloid Inter Sci 44:330
8. Williams R, Crandall RS, Wojtowicz PJ (1976) Phys Rev Lett 37:348
9. Mitaku S, Ohtsuki T, Kishimoto A, Okano K (1980) Biophys Chem 11:411
10. Lindsay HM, Chaikin PM (1982) J Chem Phys 76:3774
11. Aastuen DJW, Clark NA, Cotter LK, Ackerson BJ (1986) Phys Rev Lett 57:1733
12. Pusey PN, van Megen W (1986) Nature 320:340
13. Russel WB, Saville DA, Schowalter WR (1989) Colloidal dispersions. Cambridge University Press, Cambridge
14. Stevens MJ, Falk ML, Robins MO (1996) J Chem Phys 104:5209
15. Okubo T (1987) J Chem Phys 86:2394
16. Okubo T (1994) Langmuir 10:3529
17. Yoshinaga K, Chiyoda M, Ishiki H, Okubo T (2002) Colloid Surface 204:285
18. Asher SA, Holtz J, Liu L, Wu Z (1994) J Am Chem Soc 116:4997
19. Liu L, Li P, Asher SA (1999) J Am Chem Soc 121:4040
20. Hanabusa K, Shirai H (1998) Kobunshi Ronbunshu 55:585
21. Hurd AJ, Clark NA, Mockler RC, O'Sullivan WJ (1982) Phys Rev A 26:2869
22. Joanny JF (1979) J Colloid Interface Sci 71:622
23. Dubois-Violette E, Pieranski P, Rothen F, Strzelecki L (1980) J Phys (Paris) 41:369
24. Benzing DW, Russel WB (1981) J Colloid Interface Sci 83:178
25. Medebach M, Palberg T (2003) J Chem Phys 119:3360
26. Fujita H, Ametani K (1977) Jpn J Appl Phys 16:1907
27. Fujita H, Ametani K (1979) Jpn J Appl Phys 18:753
28. Tomita M, van de Ven TGM (1984) J Opt Soc Am A1:1907
29. Tomita M, van de Ven TGM (1985) J Phys Chem 89:1291
30. Okubo T (1987) J Chem Soc, Faraday T 83:2487
31. Okubo T (1988) J Chem Soc, Faraday T 84:3377
32. Okubo T, Tsuchida A, Okada S, Kobata S (1998) J Colloid Inter Sci 199:83
33. Tsuchida A, Taniguchi T, Tanahashi T, Okubo T (1999) Langmuir 15:4203
34. Tsuchida A, Shibata K, Okubo T (2003) Colloid Polym Sci 281:1104
35. Jennings BR, Stoylov SP (1992) (eds) Colloid and Electro-Optics, Inst Phys Pub, Bristol
36. Stoylov SP (1992) Colloids and electro-optics. Theory, techniques, applications, Academic, London
37. Okubo T, Tsuchida A, Tanahashi T, Iwata A (1998) J Colloid Inter Sci 207:130
38. Okubo T, Tsuchida A, Iwata A, Tanahashi T (1999) Colloids Surface 148:87
39. Okubo T, Tsuchida A, Tanahashi T, Iwata A, Okada S, Kobata S, Kobayashi K (1999) Colloids Surface 149:431
40. Tsuchida A, Kuzawa M, Okubo T (2002) Colloids Surface 209:235
41. Okubo T (1986) J Chem Soc, Faraday T 82:3163
42. Okubo T (1986) J Chem Soc, Faraday T 82:3175
43. Stoimenova M, Dimitrov V, Okubo T (1996) J Colloid Inter Sci 184:106
44. Okubo T, Kimura H, Hatta T, Kawai T (2002) Phys Chem Chem Phys 4:2260